ChemComm

RSC Publishing

COMMUNICATION

View Article Online
View Journal | View Issue

Cite this: *Chem. Commun.*, 2013, **49**, 9344

Received 10th July 2013,
Accepted 12th August 2013

DOI: 10.1039/c3cc45175e

www.rsc.org/chemcomm

Single source precursor routes for synthesis of PdTe nanorods and particles: solvent dependent control of shapes†

Kamal Nayan Sharma, Hemant Joshi, Alpesh K. Sharma, Om Prakash and Ajai K. Singh*

The PdTe NPs (hexagonal) and nanorods (first example) have been synthesized for the first time from single source precursors (SSPs), $[Pd(L1)Cl_2]$ (1) and $[Pd(L2)Cl]BF_4$ (2) [L1, 4-bromo-1-[2-(4-methoxyphenyltellanyl)ethyl]-1*H*-pyrazole; L2, bis-[2-(4-bromopyrazol-1-yl)-ethyl]telluride], by their thermolysis in an OA–ODE mixture (1 : 1) and TOP respectively. The composition of the PdTe phase does not change with SSP/solvent. Complex 2 gives small size nanostructures.

Metal tellurides and elemental tellurium are well-known semiconductors having a narrow band-gap energy at room temperature. They exhibit interesting properties,[1–5] *viz.* unique photoconductivity, non-linear optical, high thermoelectric and piezoelectric response, and have potential for applications in gas sensing, topological insulators, optoelectronic, photonic crystal field-effect, self-developing holographic recording, radiative cooling and field-effect devices. Currently, there is considerable interest in nanocrystals of metal chalcogenides due to their extensive applications in catalysis[6–11] and low resistance ohmic contacts of semiconducting electronic devices.[8] Palladium telluride nanocrystals having application as a catalyst for methanol electro-oxidation[12] also behave as a strongly coupled superconductor.[13] However, synthesis of high-quality nanostructures of PdTe is little explored, particularly in comparison to those of other semiconducting materials.[14–16] The methods reported for their preparation so far suffer from one or more of the following limitations. (i) Size of NPs formed varies over a wide range. (ii) The sources of palladium and tellurium are separate. (iii) Sophisticated physical technique has to be invoked. (iv) High temperature is essential. Thus there is interest in the synthesis of PdTe NPs without the use of exotic techniques, extreme conditions and dual sources currently. Numerous advantages have been ascribed to SSP based procedures over the multi-source synthetic routes. The SSP is generally used in solution at moderate temperature and thus the issues related to air and moisture instability of precursors (at higher temperature) become insignificant with SSP. The handling becomes easy at low operation temperatures and toxicity risks are comparatively reduced. The presence of only one precursor molecule in the supply stream reduces the likelihood and extent of pre-reaction and the associated contamination. Ligand designing is a tool available in the case of SSP, which gives a degree of control of the composition, morphology and the level of impurities in the final product. The work-up procedures are simple in the case of thermolysis of SSP, as organic bi-products can be easily removed by filtration or centrifugation. Thermal decomposition of complexes containing Pd–Te bond(s) in a molecule may result in nanocrystals of PdTe. Metal complexes of a number of tellurium ligands have been used as SSPs for the synthesis of nanosized binary metal tellurides, such as SnTe, PbTe, ZnTe and CdTe.[17,18] However, to the best of our knowledge, there is not a single report on the synthesis of PdTe nanocrystals by thermal decomposition of a SSP in solution. It was therefore thought to be worthwhile to develop a SSP based easy method for the synthesis of high quality and defect free PdTe nanostructures. The SSP based route is often considered less obnoxious than the multiple source one because of an intrinsic control of reactivity and stoichiometry.[19,20] We have developed two novel SSPs (Pd-complexes of bidentate and tridentate hybrid organotellurium ligands, Scheme 1). For synthesis of these ligands and their Pd-complexes a previously reported[10] strategy adopted in the case of their S/Se analogues has been used. The two SSP complexes **1** and **2** upon subsequent decomposition in solution generate PdTe nanostructures (nanorods and hexagonal nanoparticles) (Scheme 2) of high purity. Palladium(II) complex **1** was prepared by refluxing **L1** directly with $[Pd(CH_3CN)_2Cl_2]$ in CH_3CN. For the synthesis of complex **2**, ligand **L2** was first treated with $[Pd(CH_3CN)_2Cl_2]$ in CH_3CN under reflux followed by addition of solid $AgBF_4$. The precipitated AgCl was filtered off through Celite (for more details, see ESI†). Complexes **1** and **2** upon thermolysis at 220 °C in trioctylphosphine (TOP) have formed PdTe nanorods. In the mixture of oleic acid (OA) and 1-octadecene (ODE) (1 : 1), thermolysis of both the complexes at 220 °C gave PdTe hexagonal NPs.

Both the ligands (**L1** and **L2**) and Pd-complexes **1**/**2** have been characterized with ^1H, $^{13}C\{^1H\}$ and $^{125}Te\{^1H\}$ NMR spectra.

Department of Chemistry, Indian Institute of Technology Delhi, New Delhi 110016, India. E-mail: aksingh@chemistry.iitd.ac.in, ajai57@hotmail.com; Fax: +91-01-26581102; Tel: +91-011-26591379

† Electronic supplementary information (ESI) available: NMR and mass spectra, crystal structure data, SEM–EDX images, PXRD, and TEM images. CIF for **1** and **2**. CCDC 949105 and 949106. For ESI and crystallographic data in CIF or other electronic format see DOI: 10.1039/c3cc45175e

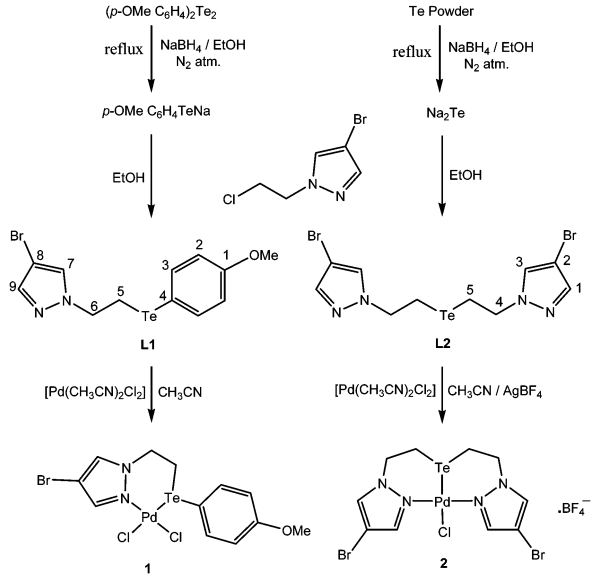

Scheme 1 Synthesis of ligands and Pd-complexes.

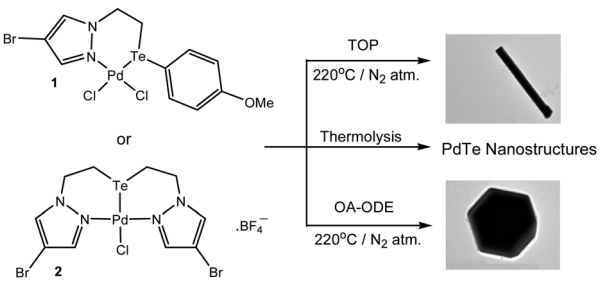

Scheme 2 Synthesis of PdTe nanostructures.

The $^{125}Te\{^1H\}$ NMR spectra of ligands (**L1** and **L2**) and their complexes (**1** and **2**) are given in Fig. S14–S17 of ESI.†

A singlet was observed at 457.1 and 238.6 ppm, respectively, in $^{125}Te\{^1H\}$ NMR spectra of **L1** and **L2**. These signals in the $^{125}Te\{^1H\}$ NMR spectra of **1** and **2** appear to be shifted to higher frequencies by 226.8 and 459.3 ppm, respectively, with respect to those of free **L1** and **L2**, implying coordination of Te with palladium. The ^1H and $^{13}C\{^1H\}$ NMR spectra (see ESI,† Fig. S6–S13) of **L1**/**L2** and their complexes **1**/**2** have been found to be consistent with their molecular structures (Scheme 1). The signals of C5 in $^{13}C\{^1H\}$ NMR spectra of **1** and **2** are at higher frequency (11.4–15.5 ppm) with respect to those of free ligands. The mass spectra of ligands and complexes were found to be characteristic of their structures (see ESI† for assignments, Fig. S18–S21). The single crystal structures of complexes **1** and **2** have been solved. Their crystal and refinement data are given in Table S1 of ESI.† In Fig. 1 and 2 their ORTEP diagrams are given with Pd–Te bond lengths consistent with earlier reports[21] (see ESI,† Table S2 for more bond length/angle values and Table S3 and Fig. S4–S5 for weak interactions).

The NPs were characterized by powder XRD, SEM-EDX and TEM. In Fig. 6 the powder X-ray diffraction (PXRD) pattern of presently synthesized NPs of PdTe is shown and it is sharp in nature. The comparison of the present PXRD pattern with those of standard phases suggests that the phase of present PdTe NPs has a hexagonal structure (JCPDS 89-2016). The morphology of present

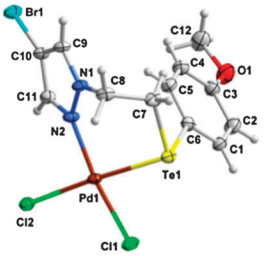

Fig. 1 Thermal ellipsoid diagram of **1** with ellipsoids at the 30% probability level. Bond length Pd–Te 2.512(6) Å.

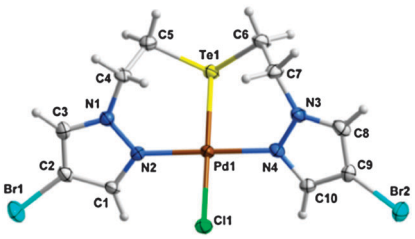

Fig. 2 ORTEP diagram of **2** with ellipsoids at the 30% probability level; BF_4^- is omitted for clarity. Bond length Pd–Te 2.531(10) Å.

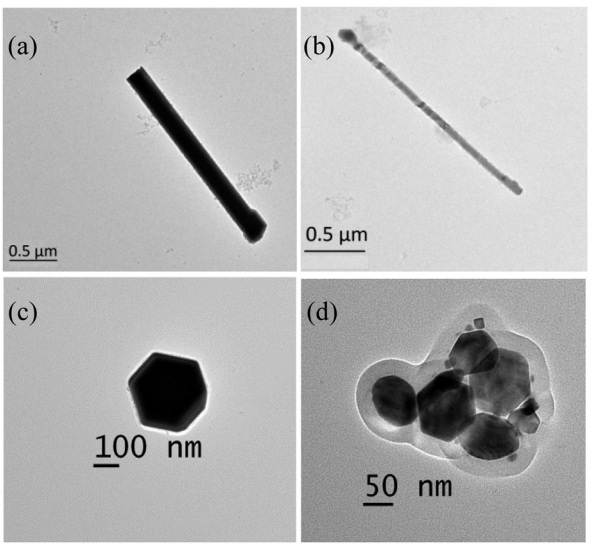

Fig. 3 TEM images of PdTe NPs obtained from (a) **1** in TOP, (b) **2** in TOP, (c) **1** in OA–ODE, (d) **2** in OA–ODE.

PdTe NPs was examined with TEM recorded at room temperature. The nanostructures (Fig. 3 and 4) obtained from **1** and **2** (in TOP) are cubic rod shaped and those prepared in OA : ODE (1 : 1) are almost hexagonal. The wide range TEM images are given in ESI† (Fig. S1) and support the purity of NPs. The TEM photographs recorded after storing the sample for two months indicate some aggregation (ESI,† Fig. S2). The sizes of NPs are shown in Table 1. The energy-dispersive X-ray spectra from SEM (Fig. S22–S25, in ESI†) indicate the presence of Pd and Te atoms in NPs obtained from **1** and **2** (nearly in a 1 : 1 ratio).

The histogram of sizes of nanostructures is given in ESI† (see Fig. S3). The size of hexagonal NPs is between 10–45 nm. The longest nanorods have size 1.8 to 2.0 μm. Kim *et al.*[24] have reported strong dependence of formation of the nanocrystals on

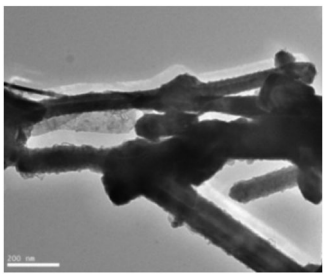

Fig. 4 TEM image of cubic PdTe nanorods.

Table 1 Size-parameters of nanostructures

	In TOP (nanorod)		In OA–ODE (hexagonal NP)	
SSP	Length (nm)	Diameter (nm)	Length (nm)	Edge length (nm)
1	2175	217	296	146–167
2	2027	71	96	45–57

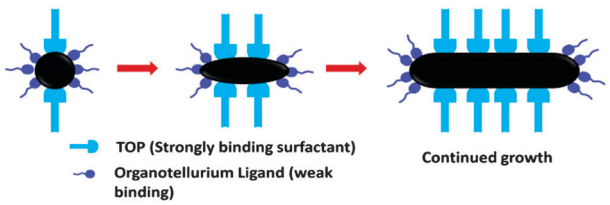

Fig. 5 Proposed growth mechanism for nanorod formation.

the chemical composition of the precursor molecule and reaction temperature. The shape of nanostructure depends on the coordinating ability of the surfactant.[22] The strongly coordinated ones do not allow equal growth in all directions. The growth in one direction results in shapes like rod.[23] Thus in our case due to the presence of strongly coordinating TOP growth is in one preferential direction only resulting in the formation of nanorods (Fig. 5). This is supported by the work of Hyeon *et al.*[22] The weak ligating power of the OA–ODE mixture results in hexagonal NPs.

The dependence of shapes of nanocrystals prepared by thermolysis on the solvent used has been noticed in few cases recently. The synthesis of shape-selective monodisperse hexagonal Sb_2Te_3 nanoplates by thermal decomposition of SSP $(Et_2Sb)_2Te$ has been reported recently by Schulz *et al.*[25] The formation of these nanoplates is independent of the temperature but the concentration of the capping agent strongly influences the size of resulting plates. Recently the influence of solvent and anions of SSP has been reported on the synthesis of Ag_2Se and AgBr NPs by us.[26] The results given in this communication indicate that chemical composition of the present nanostructured phase is independent of a single source precursor molecule and solvent used. However, the morphology of the generated NPs strongly depends on solvent. The thermolysis of both **1** and **2** in TOP gives nanorods of the PdTe phase. On the other hand in OA : ODE (1 : 1) PdTe NPs have hexagonal morphology. However chemical composition of SSP influences the dimensions of nanostructures, in both the solvents tridentate ligand based SSP gives nanostructures smaller in size relative to those obtained from SSP having a bidentate ligand (see Table 1). In summary both the complexes **1** and **2** are SSPs for PdTe nanostructures as their thermolysis in TOP gives cubic PdTe nanorods whereas in OA : ODE (1 : 1) results in hexagonal PdTe NPs.

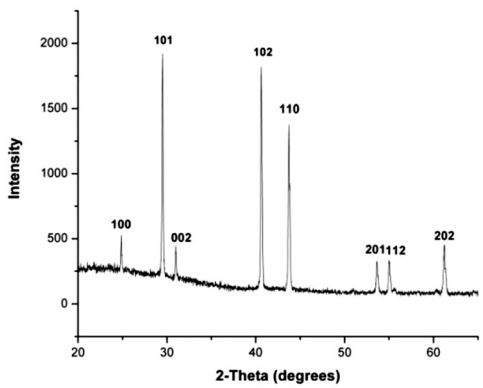

Fig. 6 PXRD of PdTe NPs.

Department of Science and Technology, Council of Scientific and Industrial Research and University Grants Commission New Delhi (India) supported this work through projects and JRF/SRF awards to KNS and AS (CSIR) and HJ and OP (UGC).

Notes and references

1 Y. Wang, Z. Y. Tang, P. Podsiadlo, Y. Elkasabi, J. Lahann and N. A. Kotov, *Adv. Mater.*, 2006, **18**, 518.
2 D. Kong and Y. Cui, *Nat. Chem.*, 2011, **3**, 845.
3 D. Kong, Y. Chen, J. J. Cha, Q. Zhang, J. G. Analytis, K. Lai, Z. Liu, S. S. Hong, K. J. Koski, S.-K. Mo, Z. Hussain, I. R. Fisher, Z.-X. Shen and Y. Cui, *Nat. Nanotechnol.*, 2011, **6**, 705.
4 K. Wang, H. W. Liang, W. T. Yao and S. H. Yu, *J. Mater. Chem.*, 2011, **21**, 15057.
5 P. Tangney and S. Fahy, *Phys. Rev. B*, 2002, **65**, 054302.
6 L. Y. Chiang, J. W. Sioirczeweki, R. Kastrup, C. S. Hsu and R. B. Upasani, *J. Am. Chem. Soc.*, 1991, **113**, 6574.
7 S. Eijsbouts, V. H. J. DeBeer and R. Prins, *J. Catal.*, 1988, **109**, 217.
8 S. Dey and V. K. Jain, *Platinum Met. Rev.*, 2004, **48**, 16.
9 H. Joshi, K. N. Sharma, A. K. Sharma, O. Prakash and A. K. Singh, *Chem. Commun.*, 2013, **49**, 7483.
10 K. N. Sharma, H. Joshi, V. V. Singh, P. Singh and A. K. Singh, *Dalton Trans.*, 2013, **42**, 3908.
11 K. N. Sharma, H. Joshi, A. K. Sharma, O. Prakash and A. K. Singh, *Organometallics*, 2013, **32**, 2443.
12 H.-H. Li, S. Zhao, M. Gong, C.-H. Cui, D. He, H.-W. Liang, L. Wu and S.-H. Yu, *Angew. Chem., Int. Ed.*, 2013, **52**, 1.
13 A. B. Karki, D. A. Browne, S. Stadler, J. Li and R. Jin, *J. Phys.: Condens. Matter*, 2012, **24**, 055701.
14 F. Gao, Q. Lu and D. Zhao, *Nano Lett.*, 2003, **3**, 85.
15 V. M. Huxter, T. Mirkovic, P. S. Nair and G. D. Scholes, *Adv. Mater.*, 2008, **20**, 2439.
16 Y. Du, B. Xu, T. Fu, M. Cai, F. Li, Y. Zhang and Q. Wang, *J. Am. Chem. Soc.*, 2010, **132**, 1470.
17 J. S. Ritch, T. Chivers, M. Afzaal and P. O'Brien, *Chem. Soc. Rev.*, 2007, **36**, 1622.
18 T. Chivers, J. S. Ritch, S. D. Robertson, J. Konu and H. M. Tuononen, *Acc. Chem. Res.*, 2010, **43**, 1053.
19 P. O'Brien, J. R. Walsh, I. M. Watson, L. Hart and S. R. P. Silva, *J. Cryst. Growth*, 1996, **167**, 133.
20 M. A. Malik, M. Afzaal and P. O'Brien, *Chem. Rev.*, 2010, **110**, 4417.
21 P. Singh, D. Das, A. Kumar and A. K. Singh, *Inorg. Chem. Commun.*, 2012, **15**, 163.
22 J. Park, B. Koo, K. Y. Yoon, Y. Hwang, M. Kang, J.-G. Park and T. Hyeon, *J. Am. Chem. Soc.*, 2005, **127**, 8433, and reference therein.
23 J. Zhang, S. Jin, H. C. Fry, S. Peng, E. Shevchenko, G. P. Wiederrecht and T. Rajh, *J. Am. Chem. Soc.*, 2011, **133**, 15324, and references therein.
24 G. Gupta and J. Kim, *Dalton Trans.*, 2013, **42**, 8209.
25 S. Schulz, S. Heimann, J. Friedrich, M. Engenhorst, G. Schierning and W. Assenmacher, *Chem. Mater.*, 2012, **24**, 2228.
26 H. Joshi, K. N. Sharma, V. V. Singh, P. Singh and A. K. Singh, *Dalton Trans.*, 2013, **42**, 2366.